We intend to design a microchip with a simpler serial bus architecture that includes Pt/Au stacked bump electrodes.

limits the usable power of the device. The operation is described in detail in [43] and is briefly mentioned here. The data transaction is based on packets as shown in Figure 12(b). The packet is transmitted on a serial bus line, which is a physical connection between the microchips. A packet consists of an 8-b address bit field followed by an 8-b data bit field. The address assigns one of 254 microchips, and the data sets the stimulus amplitude parameters. After receiving two packets, the microchip is activated for photodetection and outputs stimulus currents; the pulse duration is the same as that of the clock as shown in Figure 12(b). Figure 12(c) shows experimental results of operation for three microchips, denoted as

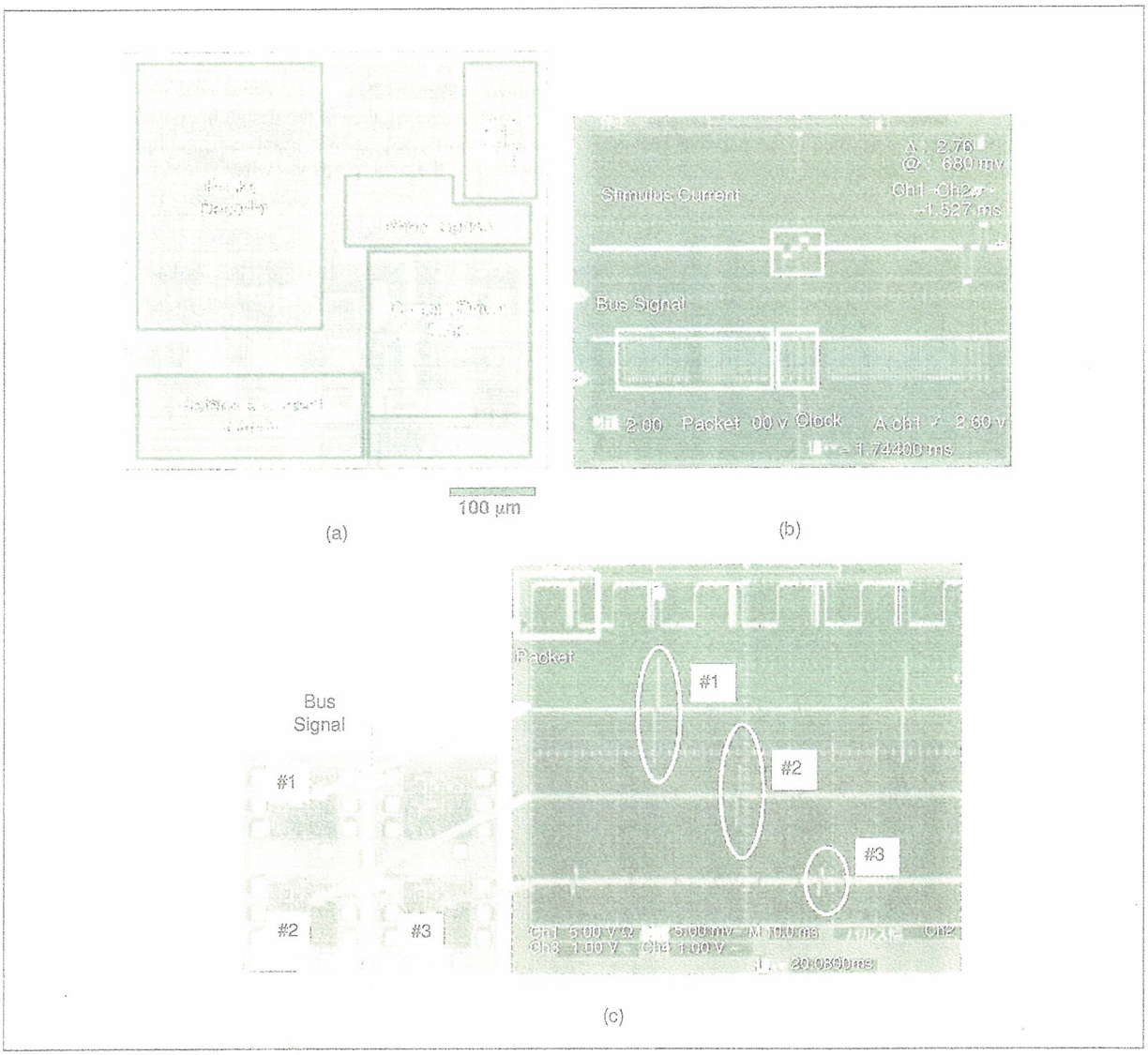

Fig. 12. Microchip-based stimulator with serial bus architecture (46). (a) Microphotograph of the fabricated microchip. Experimental results of (b) oscilloscope waveforms of the bus signal and the stimulus signal. (c) Oscilloscope waveforms of packet and the stimulus signals for #1, #2, and #3 microchips. The corresponding positions of the microchips are shown.

#1, #2, and #3. According to the bus signals, the three microchips produce different output current pulses.

The present microchip design mainly focuses on circuit architecture, and thus the device is not integrated with any electrodes. In the next step, we intend to design a microchip with a simpler serial bus architecture that includes Pt/Au stacked bump electrodes.

Conclusions

We have developed Si-LSI-based smart neural stimulators for retinal prosthesis. The application of LSI technologies confers benefits such as versatility, signal integrity, and compactness but requires a dedicated process for the integration and packaging of electrodes with the standard LSI structure. For this purpose, we have developed a Pt/Au stacked bump electrode stimulator with epoxy molding, which is suitable for forming on standard LSI chips and is effective in stimulating retinal cells. This stimulator has been evaluated in saline solution and in an in vivo experiment using detached frog retina. The positive results obtained suggest its potential in retinal prosthesis.

In summary, we have demonstrated a flexible and extendable microchip-based stimulator in which a number of microchips are distributed on a flexible polyimide substrate. Two types of such a microchip-based stimulator have been prepared: a broadcast type and a serial bus type. Both types demonstrate fundamental operations and show promising capability. In the next stage, we are planning to implant our developed microchip-based stimulator in animals to further confirm the possibility of application to human retinal prosthesis.

Acknowledgments

The authors would like to thank Prof. Tetsuya Yagi of Osaka University for the valuable discussion of in vitro experiments, Kazuaki Nakauchi of Osaka University for the semichronic data of the implanted stimulator, and Hiroyuki Tashiro of Kyushu University, Kenzo Shodo and Hiroyuki Kanda of Vision Institute, Nidek Co. Ltd. for the valuable discussion of electrodes. They also wish to thank Dr. Shigeru Nishimura and Naoko Tsunematsu of Tokyo Research Center, Nidek Co. Ltd. for their continuous encouragement and valuable discussion. This work was partly supported by the New Energy Development Organization (NEDO) of Japan ("Artificial Vision System," Prof. Y. Tano, project leader), and by Health and Labor Sciences Research Grants, Japan (Prof. Y. Tano, principal investigator).

Jun Ohta received the B.E., M.E., and Dr. Eng. degrees in applied physics, all from the University of Tokyo, Japan, in 1981, 1983, and 1992, respectively. In 1983, he joined Mitsubishi Electric Corporation, Hyogo, Japan, where he has been engaged in the research on optoelectronic integrated circuits, optical neural networks, and artificial retina chips. From 1992–1993, he was a visiting researcher in Optoelectronics Computing Systems Center, University of Colorado at Boulder. In 1998, he has been an associate professor at Graduate School of Materials Science, Nara Institute of Science and Technology (NAIST), Nara, Japan, and in 2004, he has been the professor of NAIST. His current research interests include vision chips, complementary metal oxide semiconductor image sensors, retinal prosthesis devices, biophotonic large-scale-integrations (LSIs), and integrated photonic devices.

He received the Best Paper Award of the Institute of Electronics, Information, and Communication Engineers IEICE Japan in 1992, the Ichimura Award in 1996, and the National Commendation for Invention in 2001. He is a member of the Japan Society of Applied Physics, the Institute of Electronics, Information and Communication Engineers of Japan, the Institute of Image Information and Television Engineers of Japan, Japanese Society for Medical and Biological Engineering, the Institute of Electronic and Electronics Engineers, and the Optical Society of America.

Takashi Tokuda received his B.S. and M.S. degrees in electronic engineering from Kyoto University, Kyoto, Japan, in 1993 and 1995, respectively. He received his Dr. Eng. degree in materials engineering from Kyoto University in 1998. He has been an assistant professor in the Graduate School of Materials Science, Nara Institute of Science and Technology, since 1999.

He has been working on photonic materials science and photonic device engineering. His research interests include CMOS image sensors, retinal prosthesis devices, bioimaging sensors, and biosensing devices. He is a member of the Japan Society of Applied Physics, and the Institute of Electronics, Information and Communication Engineers of Japan.

Keiichiro Kagawa received his B.E. degree in applied physics from Osaka University, Japan, in 1996. He received his M.E. and Dr. Eng. degrees in material and life science in 1998 and 2001, respectively. From 1995–2001, he was engaged in research on optical packaging and prototyping of optoelectronic parallel computers. Since 2001, he has been an assistant professor at the Nara Institute of Science and Technology, Nara, Japan.

His research interests include complementary metal oxide semiconductor image sensors, vision chips, and optoelectronic systems. He is a member of the Japan Society of Applied Physics, the Institute of Image Information and Television Engineers of Japan, and the IEEE.

Tetsuo Furumiya received the B.S. degree in mechanical engineering from Kansai University, Osaka, Japan, and the M.S. degree from Nara Institute of Science and Technology, Nara, Japan, in 2001 and 2003, respectively. Currently, he is working toward the Ph.D. degree at Nara Institute of Science and Technology.

Akihiro Uehara received the B.S. degree in electrical engineering from Osaka University, Japan in 1997. He received M.S. and Dr. Eng degrees from Nara Institute of Science and Technology, Nara, Japan, in 2000 and 2005, respectively.

In 2002, he joined the Nidek Vision Institute, Nidek Co., Ltd., Japan, where he has been engaged in the research of artificial vision prosthetic devices. His research interest is in complementary metal oxide semiconductor sensors and mixed-signal circuit design.

Yasuo Terasawa received the B.S. degree in applied physics from Tohoku University, Japan, in 1996, and an M.S. degree in information science from Tohoku University, Japan, in 1998. He joined Nidek Co., Ltd., Japan in 2001, working on the development of the retinal prosthesis. His research includes electrode technology, implantable electrical systems, and psychophysical evaluation of the prosthetic vision.

Motoki Ozawa received the B.E. degree in chemical engineering from Nagoya University, Japan, in 1985. He received M.S. degree in optics from the University of Rochester, New York, in 1987.

In 1988, he joined Dai Nippon Printing Co., Ltd., Japan, where he participated in commercialization of a digital proof printer and an electrical publishing system. In 1992, he joined Nidek Co., Ltd., Japan, where he worked on the research and development (R&D) of an excimer laser corneal surgery system. In 2003, he has been a director of the R&D division of Nidek, and since 2005, he has been a vice president of Nidek.

Takashi Fujikado is a professor of applied visual science at Osaka University Medical School, Japan. He received the B.S. and M.E. degrees from Tokyo University, Tokyo, Japan, in 1976 and 1978, respectively. He received the M.D. and Ph.D. degrees from Osaka University in 1982 and 1989, respectively.

Since joining in the department of Ophthalmology, Osaka University Medical School in 1985, he has been engaged in the research and clinical works on pediatric ophthalmology and neuro-ophthalmology. Currently, he is a member of Japanese Consortium for Artificial Retina and is engaged in the functional assessment of artificial retina.

Yasuo Tano is the professor and chairman of the Department of Ophthalmology at Osaka University Medical School as well as the vice president of the Osaka University Hospital, Japan. He is the president of the Japanese Ophthalmological Society that holds more than 13,000 members. He is currently the president of Asia-Pacific Academy of Ophthalmology, which covers an area with more than half of world population. He is the executive editor of the Japanese Journal of Ophthalmology and is a member of many international editorial boards of prominent peer-review journals. He is also a member of the International Council of Ophthalmology, the Advisory Committee for the International Council of Ophthalmology, the Academia Ophthalmologica Internationalis (Chair V) and the Executive Committee for the Club Jules Gonin and is a charter member of the International Council of Ophthalmology Foundation.

He received his M.D. from Osaka University Medical School in 1972. After completing his residency in Japan, he became a vitreoretinal research fellow at Bascom Palmer Eye Institute, Miami, Florida, in 1977 and then at Duke Eye Center, Durham, North Carolina, in 1978. Tano has authored and coauthored over 550 English and Japanese publications in various fields of ophthalmology and has written or edited over 50 books and chapters on related topics. Tano has delivered many important lectures both domestically and internationally, including the Sir Norman McAllister Gregg Lecture at the 2000 Annual Meeting of the Royal Australian and New Zealand College of Ophthalmologists, the Pyron Lecture at the 19th Annual Meeting of the Vitreous Society, and the LIX Jackson Memorial Lecture.

Tano was one of the first to perform vitrectomy in Japan and has since dedicated his time in training aspiring surgeons in the field of vitreoretinal surgery. He is the pioneer in non-vitrectomised macular surgery and is one of the leading surgeons in macular translocation. He has invented many vitreoretinal instruments, which have contributed to advances in vitreoretinal surgery in the last decade.

Address for Correspondence: Jun Ohta, Graduate School of Materials Science, Nara Institute of Science and Technology, Takayama 8916-5, Ikoma, Nara 630-0101 Japan. E-mail: ohta@ms.naist.jp.

References

[1] M.A.L. Nicolelis, Ed. *Methods for Neural Ensemble Recordings*. Boca Raton, FLA: CRC Press, 1999.

[2] J. Chen, K.D. Wise, J.F. Hetke, and S.C. Bledsoe Jr., "A multichannel neural probe for selective chemical delivery at the cellular level," *IEEE Trans. Biomed. Eng.*, vol. 44, no. 8, pp. 760–769, 1997.

[3] Q. Bai, K.D. Wise, and D.J. Anderson, "A high-yield microassembly structure for three-dimensional microelectrode arrays," *IEEE Trans. Biomed. Eng.*, vol. 47, no. 3, pp. 281–289, 2000.

[4] M.O. Heuschkel, M. Fejtl, M. Raggenbass, D. Bertrand, and P. Renaud, "A three-dimensional multi-electrode array for multi-site stimulation and recording in acute brain slices," *J. Neurosci. Methods*, vol. 114, no. 2, pp. 135–148, 2002.

[5] T. Kawano, Y. Kato, M. Futagawa, H. Takao, K. Sawada, and M. Ishida, "Fabrication and properties of ultrasmall Si wire arrays with circuits by vapor-liquid-solid growth," *Sens. Actuators A, Phys.* vol. 97–98, pp. 709–715, 2002.

[6] E. Margalit, J.D. Weiland, R.E. Clatterbuck, G.Y. Fujii, M. Maia, M. Tameesh, G. Torres, S.A. D'Anna, S. Desai, D.V. Piyathaisere, A. Olivi, E. de Juan, and M.S. Humayun, "Visual and electrical evoked response recorded from subretinal electrodes implanted above the visual cortex in normal dogs under two methods of anesthesia," *J. Neurosci. Methods*, vol. 123, no. 2, pp. 129–137, 2003.

[7] S. Takeuchi, T. Suzuki, K. Mabuchi, and H. Fujita, "3D flexible multichannel neural probe array," *J. Micromech. Microeng.*, vol. 14, no. 1, pp. 104–108, 2004.

[8] T. Suzuki, D. Ziegler, K. Mabuchi, and S. Takeuchi, "Flexible neural probes with micro-fluidic channels for stable interface with the nervous system," in *Proc. 26th Int. Conf. IEEE EMBS*, San Francisco, California, 1–5 Sept. 2004.

[9] L. Johnson, F.K. Perkins, T. O'Hearn, P. Skeath, C. Merritt, J. Frieble, S. Sadda, M. Humayun, and D. Scribner, "Electrical stimulation of isolated retinal with microwire glass electrodes," *J. Neurosci., Methods*, vol. 137, no. 2, pp. 265–273, 2004.

[10] R. Rathnasingham, D.R. Kipke, S.C. Bledsoe Jr., and J.D. McLaren, "Characterization of implantable microfabricated fluid delivery devices," *IEEE Trans. Biomed. Eng.*, vol. 51, no. 1, pp. 138–145, 2004.

[11] R.J. Vetter, J.C. Williams, J.F. Hetke, E.A. Nunamaker, and D.R. Kipke, "Chronic neural recording using silicon-substrate microelectrode arrays implanted in cerebral cortex," *IEEE Trans. Biomed. Eng.*, vol. 51, no 6, pp. 896–904, 2004.

[12] K.J. Doerner, "Implantable electronic otologic devices for hearing rehabilitation," in *Handbook of Neuroprosthetic Methods*, W. Finn and P. LoPresti, Eds. Boca Raton, FLA: CRC Press, 2002, pp. 237–260.

[13] J. Georgiou and C. Toumazou, "A 126-μW cochlear chip for a totally implantable system," *IEEE J. Solid-State Circuits*, vol. 40, no. 2, pp. 430–443, 2005.

[14] M.S. Humayun, J.D. Weiland, G.Y. Fujii, R. Greenberg, R. Williamson, J. Little, B. Mech, V. Cimmarusti, G. Van Boemel, G. Dagnelie, and E. de Juan Jr., "Visual perception in a blind subject with a chronic microelectronic retinal prosthesis," *Vision Res.*, vol. 43, no. 24, pp. 2573–2581, 2003.

[15] J.F. Rizzo III, J. Wyatt, J. Loewenstein, S. Kelly, and D. Shire, "Methods and perceptual thresholds for short-term electrical stimulation of human retina with microelectrode arrays," *Invest. Ophthalmol. Vis. Sci.*, vol. 44, no. 12, pp. 5355–5361, 2003.

[16] R. Eckmiller, "Learning retinal implants with epiretinal contacts," *Ophthalmic Res.*, vol. 29, pp. 281–289, 1997.

[17] R. Hornig, T. Laube, P. Walter, M. Velikay-Parel, N. Bornfeld, M. Feucht, H. Akguel, G. Rössler, N. Altenbeld, D.L. Notarp, J. Wyatt, and G. Richard, "A method and technical equipment for an acute human trial to evaluate retinal implant technology," *J. Neural Eng.*, vol. 2, no. 1, pp. S129–S134, 2005.

[18] A.Y. Chow, V.Y. Chow, K. Packo, J. Pollack, G. Peyman, and R. Schuchard, "The artificial silicon retina microchip for the treatment of vision loss from retinitis pigmentosa," *Arch. Ophthalmol.*, vol. 122, no. 4, pp. 460–469, 2004.

[19] E. Zrenner, "Will retinal implants restore vision?," *Science*, vol. 295, pp. 1022–1025, 2002.

[20] D. Palanker, A. Vankov, P. Huie, and S. Baccus, "Design of a high-resolution optoelectronic retinal prosthesis," *J. Neural Eng.*, vol. 2, no. 1, pp. S105–S120, 2005.

[21] H. Kanda, T. Morimoto, T. Fujikado, Y. Tano, Y. Fukuda, and H. Sawai, "Electrophysiological studies of the feasibility of suprachoroidal-transretinal stimulation for artificial vision in normal and RCS rats," *Invest. Ophthal. Vis. Sci.*, vol. 45, no. 2, pp. 560–566, 2004.

[22] K. Nakauchi, T. Fujikado, H. Kanda, T. Morimoto, J.S. Choi, Y. Ikuno, H. Sakaguchi, M. Kamei, M. Ohji, T. Yagi, S. Nishimura, H. Sawai, Y. Fukuda, and Y. Tano, "Transretinal electrical stimulation by an intrascleral multichannel electrode array in rabbit eyes," *Graefes Arch. Clin. Exp. Ophthalmol.*, vol. 243, no. 2, pp. 169–174, 2005.

[23] W. Liu, P. Singh, C. DeMarco, R. Bashirullah, M. Humayun, and J. Weiland, "Semiconductor-based implantable microsystems," Chap. 6, in *Handbook of Neuroprosthetic Methods*, W. Finn and P. LoPresti, Ed. Boca Raton, FLA: CRC Press, 2002, pp. 127–161.

[24] W. Liu, K. Vichienchom, M. Clements, S.C. DeMarco, C. Hughes, E. McGucken, M.S. Humayun, E. De Juan, J.D. Weiland, and R. Greenberg, "A neuro-stimulus chip with telemetry unit for retinal prosthetic device," *IEEE J. Solid-State Circuits*, vol. 35, no. 10, pp. 1487–1497, 2000.

[25] W. Liu and M.S. Humayun, "Retinal prosthesis," in *IEEE Int. Solid-State Circuits Conf. Dig. Tech. Papers*, 2004, pp. 218–219.

[26] K. Najafi and K.D. Wise, "An implantable multielectrode array with on-chip signal processing," *IEEE J. Solid-State Circuits*, vol. 21, no. 6, pp. 1035–1986, 1986.

[27] J. Ji, K. Najafi, and K.D. Wise, "A low-noise demultiplexing system for active multichannel microelectrode arrays," *IEEE Trans. Biomed. Eng.*, vol. 38, no. 1, pp. 75–81, 1991.

[28] S.J. Tanghe and K.D. Wise, "A 16-channel CMOS neural stimulating array," *IEEE J. Solid-State Circuits*, vol. 27, no. 12, pp. 1819–1825, 1992.

[29] C. Kim and K.D. Wise, "A 64-site multishank CMOS low-profile neural stimulating probe," *IEEE J. Solid-State Circuits*, vol. 31, no. 9, pp. 1230–1238, 1996.

[30] S.C. DeMarco, W. Liu, P.R. Singh, G. Lazzi, M.S. Humayun, and J.D. Weiland, "An arbitrary waveform stimulus circuit for visual prostheses using a low area multibias DAC," *IEEE J. Solid-State Circuits*, vol. 38, no. 10, pp. 1679–1690, 2003.

[31] Q. Bai and K.D. Wise, "Single-unit neural recording with active microelectrode arrays," *IEEE Trans. Biomed. Eng.*, vol. 48, no. 8, pp. 911–920, 2001.

[32] M. Sivaprakasam, L. Wentai, M.S. Humayun, J.D. Weiland, "A variable range bi-phasic current stimulus driver circuitry for an implantable retinal prosthetic device," *IEEE J. Solid-State Circuits*, vol. 40, no. 3, pp. 763–771, 2005.

[33] T. Kawano, Y. Kato, R. Tani, H. Takao, K. Sawada, and M. Ishida, "Selective vapor-liquid-solid epitaxial growth of micro-Si probe electrode arrays with on-chip MOSFETs on Si (111) substrates," *IEEE Trans. Electron. Devices*, vol. 51, no. 3, pp. 415–420, 2004.

[34] P. Fromherz, "Neuroelectronic interfacing: Semiconductor chips with ion channels, nerve cells, and brain," in *Nanoelectronics and Information Technology*, R. Waser, Ed. New York: Wiley, 2003, pp. 781–810.

[35] B. Eversmann, M. Jenkner, F. Hofmann, C. Paulus, R. Brederlow, B. Holzapfl, P. Fromherz, M. Merz, M. Brenner, M. Schreiter, R. Gabl, K. Plehnert, M. Steinhauser, G. Eckstein, D.S.-Landsiedel, and R. Thewes, "A 128 × 128 CMOS biosensor array for extracellular recording of neural activity," *IEEE J. Solid-State Circuits*, vol. 38, no. 12, pp. 2306–2317, 2003.

[36] P.L.-Pastor, I. Mody, and J.W. Judy, "In-vivo EEG recording using a wireless implantable neural transceiver," in *Proc. 1st Int. IEEE EMBS Conf. Neural Eng.*, Capri Island, Italy, 2003, pp. 622–625.

[37] J. Deguchi, T. Watanabe, T. Nakamura, Y. Nakagawa, T. Fukushima, J.-C. Shim, H. Kurino, T. Abe, M. Tamai, and M. Koyanagi, "Three-dimensionally stacked analog retinal prosthesis chip," *Jpn. J. Appl. Phys.*, vol. 43, no. 4B, pp. 1685–1689, 2004.

[38] M. Sawan, Y. Hu, and J. Coulombe, "Wireless smart implants dedicated to multichannel monitoring and microstimulation," *IEEE Circuit Syst. Mag.*, vol. 5, no. 1, pp. 21–39, 2005.

[39] J. Ohta, N. Yoshida, K. Kagawa, and M. Nunoshita, "Proposal of application of pulsed vision chip for retinal prosthesis," *Jpn. J. Appl. Phys.*, vol. 41, no. 4B, pp. 2322–2325, 2002.

[40] K. Kagawa, K. Isakari, T. Furumiya, A. Uehara, T. Tokuda, J. Ohta, and M. Nunoshita, "Pixel design of a pulsed CMOS image sensor for retinal prosthesis with digital photosensitivity control," *Electron. Lett.*, vol. 39, no. 5, pp. 419–420, 2003.

[41] D.C. Ng, K. Isakari, A. Uehara, K. Kagawa, T. Tokuda, J. Ohta, and M. Nunoshita, "A study of bending effect on pulsed frequency modulation based photosensor for retinal prosthesis," *Jpn. J. Appl. Phys.*, vol. 42, no. 12, pp. 7621–7624, 2003.

[42] K. Kagawa, N. Yoshida, T. Tokuda, J. Ohta, and M. Nunoshita, "Building a simple model of a pulse-frequency-modulation photosensor and demonstration of a 128 × 128-pixel pulse-frequency-modulation image sensor fabricated in a Standard 0.35-μm complementary metal-oxide semiconductor technology," *Opt. Rev.*, vol. 11, no. 3, pp. 176–181, 2004.

[43] K. Kagawa, K. Yasuoka, D.C. Ng, T. Furumiya, T. Tokuda, J. Ohta, and M. Nunoshita, "Pulse-domain digital image processing for vision chips employing low-voltage operation in deep-submicrometer technologies," *IEEE J. Select. Topics Quantum Electron.*, vol. 10, no. 4, pp. 816–828, 2004.

[44] T. Furumiya, D.C. Ng, K. Yasuoka, K. Kagawa, T. Tokuda, M. Nunoshita, and J. Ohta, "Functional verification of pulse frequency modulation-based image sensor for retinal prosthesis by in vitro electrophysiological experiments using frog retina," *Biosens. Bioelectron.*, vol. 21, no. 7, pp. 1059–1068, 2006.

[45] A. Uehara, K. Kagawa, T. Tokuda, J. Ohta, and M. Nunoshita, "Back-illuminated pulse-frequency-modulated photosensor using silicon-on-sapphire technology developed for use as epi-retinal prosthesis device," *Electron. Lett.*, vol. 39, no. 15, pp. 1102–1103, 2003.

[46] A. Uehara, Y.-L. Pan, K. Kagawa, T. Tokuda, J. Ohta, and M. Nunoshita, "Micro-sized photo-detecting stimulator array for retinal prosthesis by distributed sensor network approach," *Sens. Actuators A. Phys.*, vol. 120, no. 1, pp. 78–87, 2005.

[47] T. Tokuda, Y.-L. Pan, A. Uehara, K. Kagawa, M. Nunoshita, and J. Ohta, "Flexible and extendible neural interface device based on cooperative multi-chip CMOS LSI architecture," *Sens. Actuators A Phys.*, vol. 122, no. 1, pp. 88–98, 2005.

[48] Y.-L. Pan, T. Tokuda, A. Uehara, K. Kagawa, J. Ohta, and M. Nunoshita, "A flexible and extendible neural stimulation device with distributed multi-chip architecture for retinal prosthesis," *Jpn. J. Appl. Phys.*, vol. 44, no. 4B, pp. 2099–2103, 2005.

[49] I. Li, Y. Hayashida, and T. Yagi, "Temporal properties of retinal ganglion cell responses to local trans retinal current stimuli in the frog retina," *Vision Res.*, vol. 45, no. 2, pp. 263–273, 2005.

[50] A.P. Chu, K. Morris, R.J. Greenberg, and D.M. Zhou, "Stimulus induced pH changes in retinal implants," in *Proc. 26th Int. Conf. IEEE EMBS*, San Francisco, California, U.S.A., 1–5 Sept. 2004, pp. 4160–4162.

[51] T.L. Rose and L.S. Robblee, "Electrical stimulation with Pt electrodes. VIII. Electrochemically safe charge injection limits with 0.2 ms pulses," *IEEE Trans. Biomed. Eng.*, vol. 37, no. 11, pp. 1118–1120, 1990.

[52] S.B. Brummer and M.J. Turner, "Electrical stimulation with Pt electrodes: II—estimation of maximum surface redox (theoretical non-gassing) limits," *IEEE Trans. Biomed. Eng.*, vol. 24, no. 5, pp. 440–443, 1977.

[53] S.B. Brummer and M.J. Turner, "Electrical stimulation with Pt electrodes: I. A method for determination of 'real' electrode areas," *IEEE Trans. Biomed. Eng.*, vol. 24, no. 5, pp. 436–439, 1977.

[54] J.D. Weiland and D.J. Anderson, "Chronic neural stimulation with thin-film, Iridium Oxide electrodes," *IEEE Trans. Biomed. Eng.*, vol. 47, no. 7, pp. 911–918, 2000.

[55] S.F. Cogan, T.D. Plante, J. Ehrlich, "Sputtered iridium oxide films (SIROFs) for low-impedance neural stimulation and recording electrodes," in *Proc. 26th Int. Conf. IEEE EMBS*, San Francisco, California, U.S.A., 1–5 Sept. 2004, pp. 4153–4156.

[56] W. Yang, "A wide-dynamic-range, low-power photosensor array," in *IEEE Int. Solid-State Circuits Conf. Dig. Tech. Papers*, 1994, pp. 230–231.

[57] M. Mazza, P. Renaud, D.C. Bertrand, and A.M. Ionescu, "CMOS Pixels for Subretinal Implantable Prosthesis," *IEEE Sens. J.*, vol. 5, no. 1, pp. 32–37, 2005.

INSTITUTE OF PHYSICS PUBLISHING JOURNAL OF NEURAL ENGINEERING
J. Neural Eng. 4 (2007) 1–7 UNCORRECTED PROOF

Laboratory investigation of microelectronics-based stimulators for large-scale suprachroidal transretinal stimulation (STS)

J Ohta[1], T Tokuda[1], K Kagawa[1], S Sugitani[1], M Taniyama[1], A Uehara[2], Y Terasawa[2], K Nakauchi[3], T Fujikado[3] and Y Tano[4]

[1] Graduate School of Materials Science, Nara Institute of Science and Technology, 8916-5 Takayama, Ikoma, Nara 630-0101, Japan
[2] Vision Institute, Nidek Co., Ltd, 73-1 Hamacho, Gamagori, Aichi, Japan
[3] Department of Applied Visual Science, Osaka University Graduate School of Medicine, 2-2 Yamadagaoka, Suita, Osaka, Japan
[4] Department of Ophthalmology, Osaka University Graduate School of Medicine, 2-2 Yamadagaoka, Suita, Osaka, Japan

E-mail: ohta@ms.naist.jp

Received 30 September 2006
Accepted for publication 14 December 2006
Published DD MMM 2007
Online at stacks.iop.org/JNE/4/1

Abstract

This paper describes the technological developments underlying the realization of a reliable and reproducible microchip-based stimulator with a large number of stimulus electrodes. A microchip-based stimulator with over 500 electrodes for suprachoroidal transretinal stimulation (STS) is proposed in this paper, and an example is presented. To enhance reliability and reproducibility for such a large array, we introduce a flip-chip bonding technique and place microchips on the reverse side of a substrate. A square microchip of size 600 μm was fabricated using 0.35 μm standard CMOS process technology. Twelve microchips were flip-chip bonded on a polyimide substrate through Au bumps. To evaluate the feasibility of the proposed device, we successfully fabricated a stimulator with 12 microchips and 118 electrodes made of Pt/Au bumps, and demonstrated their operation in a saline solution for 2 weeks. Also, to evaluate the device operation *in vivo*, a stimulator with one active IrO_x electrode was implanted into the scleral pocket of a rabbit and electrical evoked potential (EEP) signals with a threshold of 100 μA were obtained. We also fabricated a simulator with 64 microchips that has 576 electrodes (9 electrodes in a microchip times 64 microchips).

(Some figures in this article are in colour only in the electronic version)

1. Introduction

Several types of intraocular retinal prostheses for blind patients have been reported [1–7]. With the exception of [5], most have been characterized by a small number of electrodes. Although more than 1000 electrodes would be preferable for realizing better vision using a retinal prosthesis, we are faced with the issue of interconnection between electrodes and external lead wires when increasing the number of electrodes.

Figure 1 illustrates the methods used to realize a stimulus electrode array. The direct connection method, which is commonly used in retinal prosthetic devices, is shown in figure 1(a), where each electrode is directly connected to a lead wire. A more sophisticated method is shown in figure 1(b), where a multiplexer is employed to reduce the number of external lead wires. If the number of electrodes is increased further, it would be difficult to connect electrodes to the multiplexer due to the number of wires.

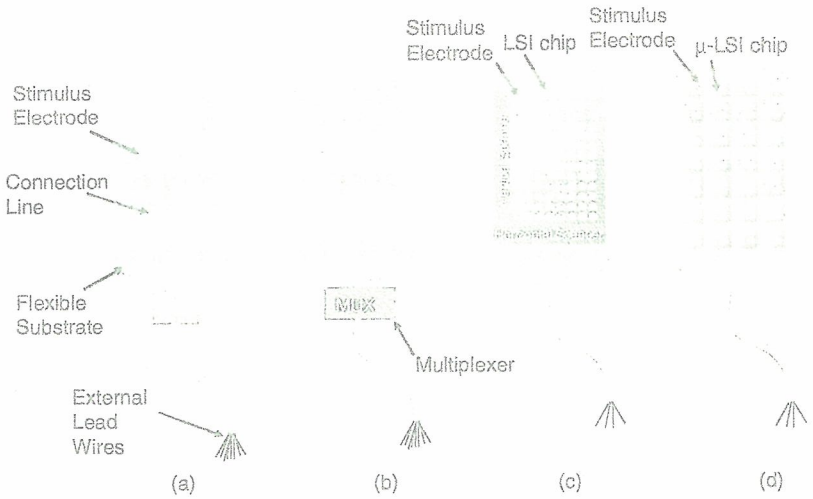

Figure 1. Illustration of several methods to realize connections between electrodes and external lead wires. (a) Direct connections between electrodes and lead wires. (b) Introducing a multiplexer to reduce the number of external lead wires. (c) An LSI chip introduced for scanning circuits. (d) Our proposed method using microchips.

It is thus preferable to introduce a large-scale integration (LSI) chip in the stimulator, as shown in figure 1(c). The LSI chip enables scanning circuits (scanners) to be integrated to reduce the number of wires. Random access can be implemented using decoder circuits instead of scanners. However, it is difficult to use an LSI chip in a retinal stimulator device. Specifically, for implantation, an LSI-based stimulator should be thin and flexible to accommodate the eye and to avoid damaging tissue. However, silicon is rigid and decreasing the thickness of the LSI chip increases the risk of breakage.

To solve this issue, we have already developed a novel smart stimulator that consists of a number of LSI-based microchips distributed on a flexible substrate, as shown in figure 1(d) [10–12]. Each microchip has several stimulus electrodes, which can be externally controlled to turn on and off through an external control circuit. In addition to resolving the interconnections issue, LSI-based stimulators offer several advantages for signal processing. To facilitate flexibility, we place several microchips on a substrate in a distributed manner.

In this paper, we propose a new structure for realizing a large electrode array. This new structure offers improved extendibility and sealing characteristics in a biological environment in comparison with our previously proposed stimulator [11]. This latest stimulator was primarily developed for suprachoroidal transretinal stimulation (STS) applications [8, 9], although it has other potential applications, such as subretinal stimulation. In addition, STS has been applied recently to RP (retinitis pgimentosa) patients [7].

This paper is organized as follows. First, we describe the design and fabrication process of the stimulator for STS. Next, the experimental results of the simulator are demonstrated. Finally, a stimulator approaching a 1000-electrode array is discussed.

2. Design and fabrication of the stimulator

2.1. Microchip design

The microchip architecture is almost the same as in [10]; it has nine stimulation pads and four input lines, including the power supply lines. However, the chip in this paper has been improved to accommodate an increased number of microchips in the stimulator. The circuits of the microchip are briefly described below. A detailed description of the integrated circuits will appear in [13].

A block diagram of the chip is shown in figure 2. Each stimulation pad is assigned a unique 4-bit address that can selectively activate one of the nine electrodes on a microchip. The four input lines are VDD, GND, CTLR and STIM. The VDD and GND lines are used for the power supply (VDD = 5 V), and control and stimulation can be achieved with only two lines: CTLR and STIM. Each of the stimulation electrodes can be selected with the number of the pulses applied on the CTLR line. This is achieved by the microchip counting the pulses applied on the CTLR line using a 10-bit address buffer. As shown in figure 2, the lower 4 bits of the address buffer are used for electrode selection and the upper 6 bits are used for chip identification. The stimulation current is provided from outside of the chip and fed into the STIM terminal. Because a precise current source can be used, the charge balance is maintained. Therefore, a capacitor for charge balance and preventing the flow of unintentional dc current to the tissues is not employed in the present design.

One of the stimulation electrodes is selected depending on the value in the lower 4 bits of the address buffer. The 6-bit address space for microchips facilitates the control of an arbitrary number of microchips (up to 64) using only one set of input lines. Consequently, the multi-chip stimulation device platform can configure a 64-chip device with 576 stimulation electrodes. To ensure flexibility, the microchip array is assembled at a pitch of 1000–1200 μm.

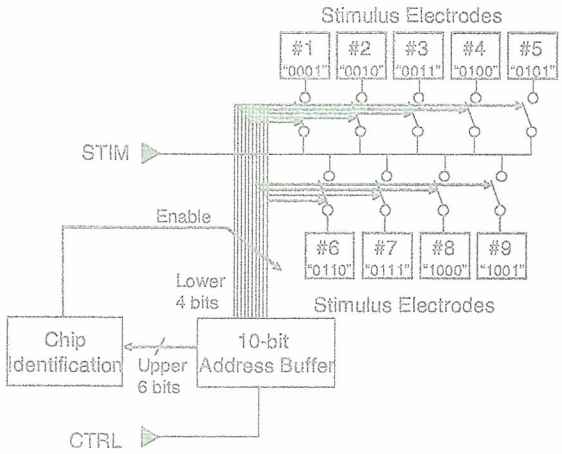

Figure 2. Block diagram of the microchip. The 4-digit number in each stimulus electrode refers to the number assigned to the electrode.

The microchips are diced from a mother chip, which is fabricated using 0.35 μm standard CMOS technology. The mother chip contains 16 microchips. Figure 3 shows microphotographs of a mother chip and a microchip measuring 600 μm × 600 μm.

2.2. *Stimulator design*

To enhance the extendibility and reliability of the stimulator for large array sizes, we propose a new stimulator design that places the microchips on the reverse side of a flexible substrate by a process called flip-chip bonding. Flip-chip bonding has not been used in the design of previous stimulators [10, 11]. The detailed fabrication process has been submitted for publication in [13]. The proposed stimulator is illustrated in figure 4. For clarity in the figure, the microchips have been placed on the substrate, but in use they are placed on the reverse side of the substrate and thus cannot be seen.

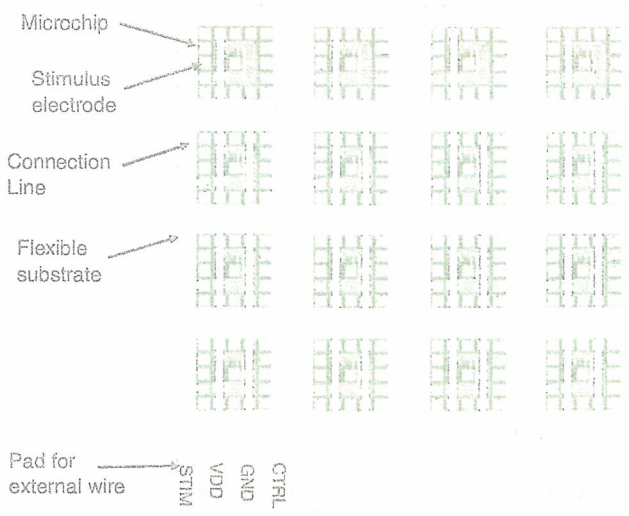

Figure 4. Illustration of the stimulator. 4 × 4 microchips are placed on a substrate. Four vertical lines for VDD, GND, STIM and CTRL connect four microchips.

For extendibility, the microchips are connected to each other such that a column can be extended vertically. Consequently, the stimulator can accommodate more microchips. All of the connection wires are placed on the reverse side of the substrate; no wires connecting microchips are necessary, which means that the stimulator is more reliable compared with previous stimulators, in which microchips were connected via wires [11].

2.3. *Fabrication process of the stimulator*

We designed and fabricated the arrayed microchip using one die. The fabrication process is shown in figure 5 and described as follows. First, grooves for separating each microchip are formed on the die. Then, connection bumps for flip-chip bonding are formed on the pads of the microchips. We use

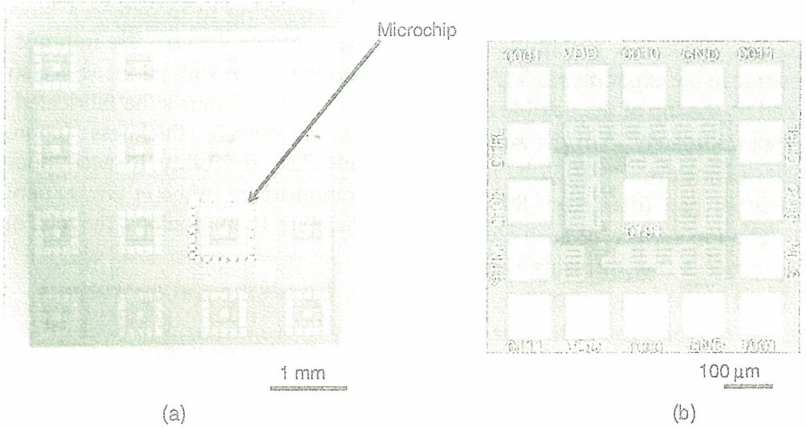

Figure 3. Microphotographs of the (a) fabricated mother chip and (b) a diced microchip. The 4-digit number in (b) is the same as that shown in figure 2.

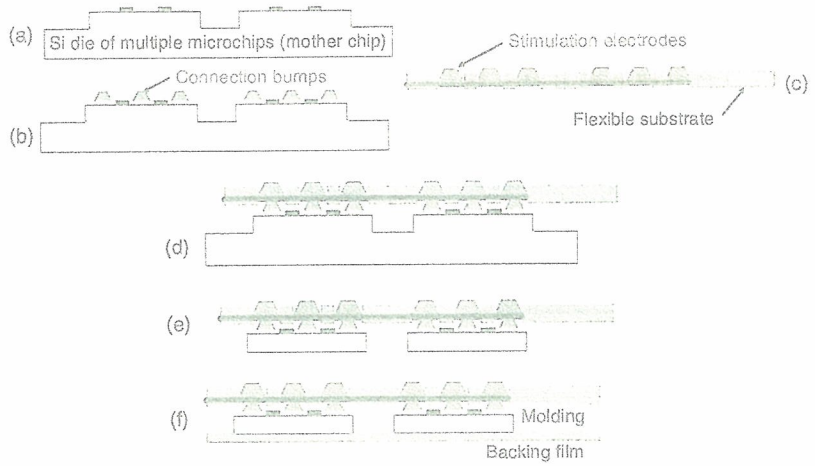

Figure 5. Fabrication process of the stimulator. (a) Grooving for separation. (b) formation of connection bumps. (c) formation of stimulation electrodes on the flexible substrate, (d) flip-chip bonding with the Si mother chip and flexible substrate, (e) microchip separation and (f) molding.

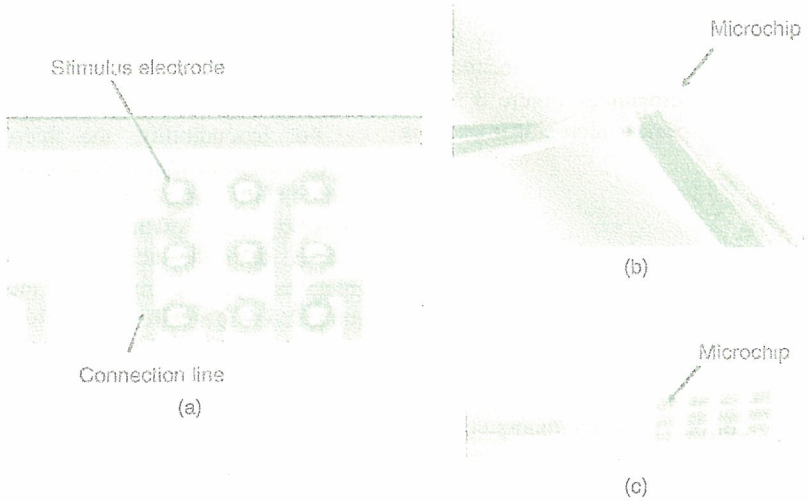

Figure 6. Microphotographs of the fabricated stimulator. (a) Close-up view of the upper surface of the fabricated stimulator. (b) Upper surface view of the stimulator to show that it can easily be bent. (c) Reverse surface view of the stimulator to show the microchips flip-chip-bonded on the substrate.

gold ball bumps as the connection bumps. Next, the die is bonded onto the reverse side of the flexible patterned substrate by the flip-chip bonding technique. A polyimide film was used for the flexible substrate in the experiments. Pt/Au bump electrodes [10] are formed on the top of the flexible substrate, each of which measures approximately 75 m$\mu\phi$. An electrode consists of a Pt top part (diameter: 70–80 μm, thickness: 20–40 μm) and a Au bottom part (diameter: 80–100 μm, thickness: 10–40 μm). The top surface of each electrode is flattened by the tamping process (i.e., pressing with a solid material).

The bottom of the die is then ground to separate each microchip completely before molding with epoxy resin and a backing film made of Teflon film. The molding material, epoxy resin, is used for sealing against moisture, which is evaluated *in vitro* in the short term, as mentioned in section 3.1. We have not yet confirmed the long-term sealing performance and biocompatibility for individual materials, although we are preparing to introduce a biocompatible epoxy resin for the molding layer. To improve the sealing performance, encapsulation with parylene is also under examination.

Figure 6 shows the fabricated stimulator. The stimulator has acceptable thickness (approximately 250 μm) and sufficient flexibility to accommodate an eyeball, which is demonstrated in the *in vivo* experiment in section 3.2. Since there are 16 microchips, the total number of electrodes is 144.

3. Fundamental operations

3.1. In vitro operation

The fabricated stimulator with Pt/Au electrodes was tested in a saline solution for several pulse conditions. Figure 7 summarizes the experimental results, which show that the stimulator can operate properly in a saline solution. The

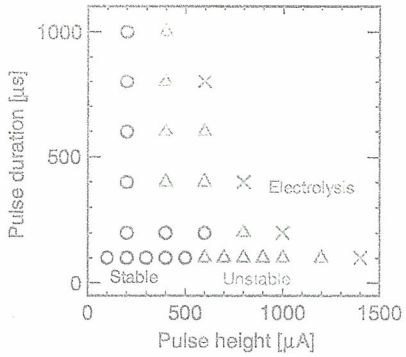

Figure 7. Operating region of the stimulator in saline solution. ○: stable condition; △: unstable condition where electrolysis occasionally occurred after some trials; ×: irreversible condition where electrolysis occurred, that is, gas bubbling was observed. Pulse is cathodic-first biphasic and cathodic, anodic and interpulse durations are the same. The repetition rate is 1 kHz.

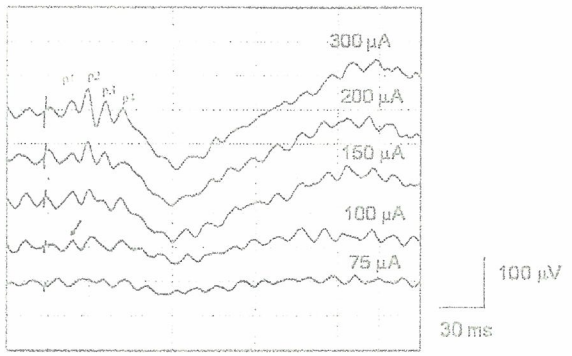

Figure 8. EEP signals, showing the parameters of the pulse current amplitude for a duration of 0.5 ms. The arrow indicates the p1 peak at the threshold.

pulse parameters used are described in the figure caption. We also confirmed that the maximum charge capacity of our electrode (Pt) is estimated approximately as 1 mC cm $^{-2}$, which is three times larger than the values cited in the literature [14]. This is presumably due to neglecting the surface roughness factor to estimate the charge capacity in our electrodes, and needs further studies. Another experiment demonstrated that the stimulator could operate for more than 2 weeks with a cathodic-first biphasic pulse of 200 μA in amplitude for both cathodic and anodic pulses with a duration of 200 μs for both pulses and interpulses at the frequency of 1 kHz. The *in vitro* results demonstrate that, in the 2 weeks of testing, the molding was leak-tight and the electrodes worked well without damage. The long-term evaluation, however, is a future issue.

3.2. *In vivo operation*

We then conducted an *in vivo* experiment in which we implanted the fabricated stimulator into the scleral pocket of a rabbit eye using an operation procedure similar to that described in [9]. In this experiment, a dummy silicon chip, which was the same size as the microchip, was used and IrO_x was formed on the Pt electrode to increase the charge capacity and ensure the effective stimulation *in vivo* environment. A dummy chip is useful for evaluating fundamental characteristics such as bending in the tissue, stimulation performance with a simple operation, and so on, in a first trial. The values of the charge capacity of the Pt and IrO_x used here are in the range of values cited in the literature [14]. The size of the electrode was the same as the stimulator that was described in the previous section. The method of recording EEP from anesthetized rabbit cortex with the stimulator in STS is as follows.

Implantation of the recording electrodes. The rabbit was anesthetized with an intramuscular injection of ketamine hydrochloride (50 mg kg^{-1}) and xylazine hydrochloride (5 mg kg^{-1}), which provided a stable anesthesia for more than 2 h. The recording electrode was a stainless-steel screw. The electrode was screwed into the skull at the area of the visual cortex to a depth of 4 mm so that the tip touched the dura mater. The reference electrode was screwed at the bregma.

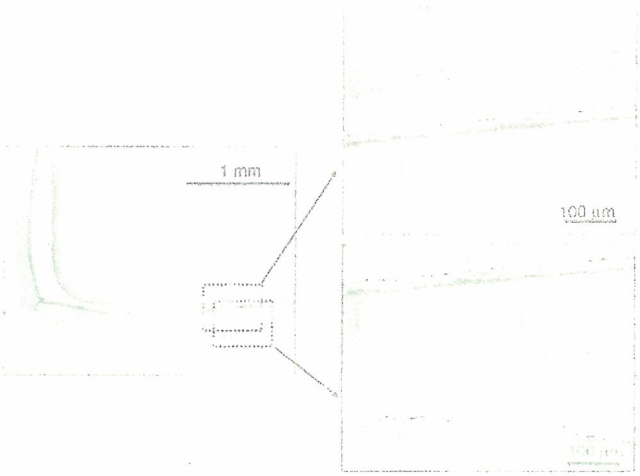

Figure 9. Histology of the retina and sclera around the electrode array.

Implantation of the stimulating electrodes. The rabbit eye was proptosed and draped with sterilized rubber cloth. After cutting the ventral conjunctiva, the exposed inferior rectus and inferior oblique muscles were cut at the insertion. Then, a 4 × 4 mm scleral pocket was made over the visual streak, which is located 10 mm dorsal to the lower corneal limbus. The electrode was inserted into that pocket and fixed with a 5-0 Dacron suture. A return electrode was inserted into the vitreous cavity. A scleral hole was made at 1 mm from the limbus with a 30-gauge needle. The electrode wire was inserted 3 mm into the vitreous and fixed by an 8-0 Vicryl suture, and a silicone tube was fixed by a 5-0 Dacron suture on the sclera.

Stimulation parameters. Monophasic 0.5 ms duration pulses with anodic polarity were used to elicit the EEPs. The stimulus currents were changed to determine threshold currents, but they did not exceed 500 μA. A power generator (A-365R; World Precision Instruments Inc., Sarasota, FL USA) was connected to an electronic pulse generator (Stimulator SEN-7203, Nihon Kohden, Shinjyuku, JAPAN).

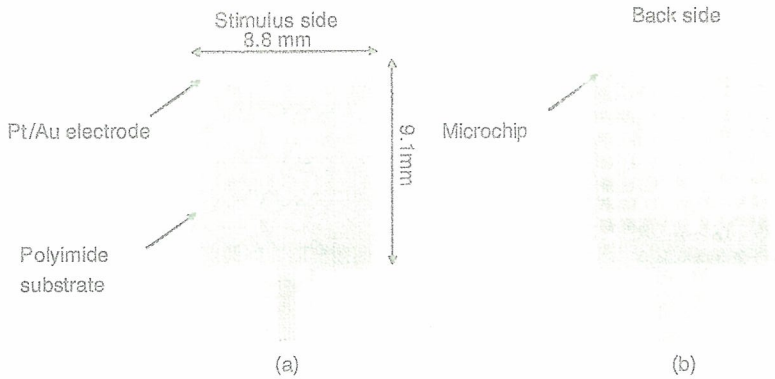

Figure 10. Photographs of the fabricated stimulator with 576 Pt/Au electrodes. (a) Upper surface view to show the 576 stimulus electrodes. (b) Reverse surface view to show the 16 microchips flip-chip bonded on the polyimide substrate.

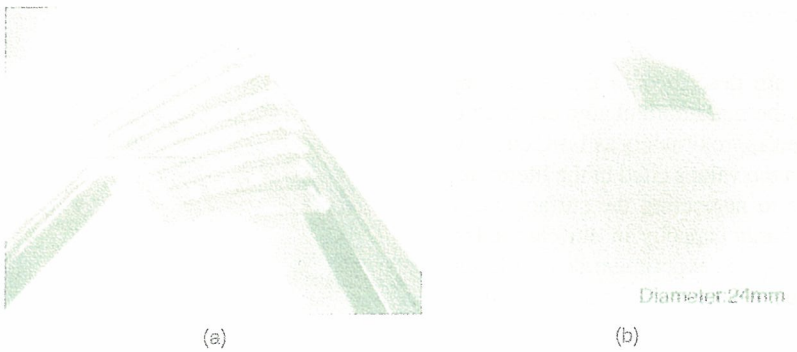

Figure 11. Photographs of the 576-electrode stimulator with vertical cutting slits. (a) By virtue of the vertical slits, the stimulator can be bent in any direction, and (b) can be fitted to a ball with the same diameter as the human eye.

Recording methods. The visual evoked potentials (VEPs) and EEPs were recorded with the Neuropac (KD-019A, Nihon Kohden) system. A flash bulb (1.2 J) was placed 15 cm from the cornea. The responses to 20 stimuli were averaged for the VEP. Then, 20 to 30 EEP responses were averaged.

Figure 8 shows the EEP experimental results, where we conclude that 'p1' is the EEP signal from the ganglion cells because of the latency of the signal. The p1 peak and other peaks after p1 are discussed in detail in [9]. From p1, the threshold is approximately 100 μA (<1 mC cm^{-2}), which is considered adequate for the charge capacity of the electrode (1–4 mC cm^{-2} [14]).

The electrode array was implanted for 2 weeks after stimulation for 1 h with the following pulse parameters: an anodic pulse with a height of 1 mA, duration of 0.5 ms and frequency of 20 Hz. As shown in figure 9, histological examination revealed that the stimulator caused only minor damage to the retinal tissue after 2 weeks.

4. A 1000-electrode stimulator

In this section, we discuss a stimulator consisting of an array approaching 1000 electrodes. In the present stimulator, the number of stimulus electrodes can be increased up to 576; the 6-bit address for microchips can be assigned to 64 microchips, and since 9 electrodes can be accommodated by each of the 64 microchips, a total of 576 electrodes can be integrated into the stimulator. It is possible to increase the number of electrodes by increasing the address bit from 6 bits to 7 bits; a 7-bit address can assign 128 microchips, which would result in 1152 electrodes in the stimulator. Another way to reach a 1000-electrode stimulator is to use two sets of the 576-electrode stimulator, thereby realizing 1152 electrodes. We fabricated a mockup stimulator, in which dummy Si chips without integration circuits were used instead of microchips. Sixty-four chips were placed on the substrate to give 576 stimulus electrodes on the stimulator, as shown in figure 10. The size of the stimulator is 8.8 mm × 9.1 mm.

By introducing vertical slits in the stimulator, it can be bent, even if the size of the stimulator is as large as that shown in figure 11(a). Figure 11(b) shows that a large stimulator such as this can be fitted to a ball with the same diameter as that of a human eye (24 mm).

Although this stimulator was designed for demonstration purposes, we believe that this method would be effective for producing large-scale STS stimulators.

5. Conclusions

We have proposed and fabricated a flip-chip type stimulator for a large number of stimulations for STS. Better extendibility

and reliability are demonstrated compared with previously proposed stimulators, and as many as 576 simulation electrodes can be realized in the fabricated device. The operation of the fabricated stimulator was tested in a saline solution and found to function within safe operation limits. A stimulator with one active IrO_x electrode on a dummy Si microchip was also implanted in the scleral pocket of a rabbit, where it operated for 2 weeks. By using the stimulator, EEP signals with thresholds of 100 μA were observed. With the intention of fabricating a 1000-electrode stimulator, we fabricated a 576-electrode stimulator with vertical slits that can be accommodated by a human eyeball.

Acknowledgments

The authors would like to thank Professor H Tashiro of Kyushu University, M Ozawa, K Shodo, H Kanda and N Tsunematsu of Nidek Co. Ltd for their valuable discussions. This work was partly supported by the New Energy Development Organisation (NEDO) of Japan ('Artificial Vision System' Project) and by a Health and Labour Sciences Research Grant, Japan.

References

[1] Humayun M S *et al* 2003 Visual perception in a blind subject with a chronic microelectronic retinal prosthesis *Vis. Res.* *43* 2573–81

[2] Liu W and Humayun M S 2004 Retinal prosthesis *IEEE Int. Solid-State Circuits Conf. Dig. Technical Papers* pp 218–9

[3] Rizzo J F III, Wyatt J, Loewenstein J, Kelly S and Shire D 2003 Methods and perceptual thresholds for short-term electrical stimulation of human retina with microelectrode arrays *Invest. Ophthalmol. Vis. Sci.* *44* 5355–61

[4] Hornig R *et al* 2005 A method and technical equipment for an acute human trial to evaluate retinal implant technology *J. Neural Eng.* 2 S129–34

[5] Chow A Y, Chow V Y, Packo K, Pollack J, Peyman G and Schuchard R 2004 The artificial silicon retina microchip for the treatment of vision loss from retinitis pigmentosa *Arch. Ophthalmol.* *122* 460–9

[6] Zrenner E, Besch D, Bartz-Schmidt K U, Gekeler F, Gabel V P, Kuttenkeuler C, Sachs H, Sailer H, Wilhelm B and Wilke R 2006 Subretinal chronic multi-electrode arrays implanted in blind patients *Invest. Ophthalmol. Vis. Sci.* *47* E-Abstract 1538

Zrenner E 2006 Subretinal chronic multi-electrode arrays implanted in blind patients *Abstract Book of Shanghai Int. Conf. Physiological Biophysics (Shanghai)* p 147

[7] Kamei M, Fujikado T, Kanda H, Morimoto T, Nakauchi K, Sakaguchi H, Ikuno Y, Ozawa M, Kusaka S and Tano Y 2006 Suprachoroidal-transretinal stimulation (STS) artificial vision system for patients with retinitis pigmentosa *Invest. Ophthalmol. Vis. Sci.* *47* E-Abstract 1537

[8] Kanda H, Morimoto T, Fujikado T, Tano Y, Fukuda Y and Sawai H 2004 Electrophysiological studies of the feasibility of suprachoroidal-transretinal stimulation for artificial vision in normal and RCS rats *Invest. Ophthal. Vis. Sci.* *45* 560–6

[9] Nakauchi K *et al* 2005 Transretinal electrical stimulation by an intrascleral multichannel electrode array in rabbit eyes *Graefes Arch. Clin. Exp. Ophthalmol.* *243* 169–74

[10] Ohta J, Tokuda T, Kagawa K, Furumiya T, Uehara A, Terasawa Y, Ozawa M, Fujikado T and Tano Y 2006 Silicon LSI-based smart stimulators for retinal prosthesis *IEEE Eng. Med. Biol. Mag.* *25* 47–59

[11] Tokuda T, Pan Y-L, Uehara A, Kagawa K, Nunoshita M and Ohta J 2005 Flexible and extendible neural interface device based on cooperative multi-chip CMOS LSI architecture *Sensors Actuators* A *122* 88–98

[12] Uehara A, Pan Y-L, Kagawa K, Tokuda T, Ohta J and Nunoshita M 2005 Micro-sized photo detecting stimulator array for retinal prosthesis by distributed sensor network approach *Sensors Actuators* A *120* 78–87

[13] Tokuda T, Sugitani S, Taniyama M, Uehara A, Terasawa Y, Kagawa K, Nunoshita M, Tano Y and Ohta J Fabrication and validation of a multi-chip neural stimulator for *in vivo* experiments toward retinal prosthesis *Japan. J. Appl. Phys.* at press

[14] Weiland J D, Liu W and Humayun M S 2005 Retinal prosthesis *Annu. Rev. Biomed. Eng.* 7 361–401

Q1

Queries

(1) Author: Please update reference [13].
(2) Author: The cost of printing a single page in colour is 475 GBP. Each additional page costs 95 GBP. Please let us know if you would like to cover this cost, or if you would prefer colour to appear in the electronic version only.

J Artif Organs (2006) 9:263–266
DOI 10.1007/s10047-006-0352-1

BRIEF COMMUNICATION

Yasuo Terasawa, MS · Hiroyuki Tashiro, MS
Akihiro Uehara, PhD · Tohru Saitoh, BS
Motoki Ozawa, MS · Takashi Tokuda, PhD
Jun Ohta, PhD

The development of a multichannel electrode array for retinal prostheses

Abstract The development of a multielectrode array is the key issue for retinal prostheses. We developed a 10 × 10 platinum electrode array that consists of an 8-μm polyimide layer sandwiched between 5-μm polymonochloro-para-xylylene (parylene-C) layers. Each electrode was formed as a 30-μm-high bump by Pt/Au double-layer electroplating. We estimated the charge delivery capability (CDC) of the electrode by measuring the CDCs of two-channel electrode arrays. The dimensions of each electrode of the two-channel array were the same as those of each electrode formed on the 10 × 10 array. The results suggest that for cathodic-first (CF) pulses, 80% of electrodes surpassed our development target of 318 μC/cm^2, which corresponds to the charge density of pulses of 500 μs duration and 200 μA amplitude for a 200-μm-diameter planar electrode.

Key words Visual prosthesis · Electrode · Charge delivery capability

Introduction

In spite of recent advances in medicine, there is no effective treatment for blindness. Recently, it has been shown that a certain percentage of retinal cells survive even in the retina of a totally blind eye,[1,2] which has encouraged the development of retinal prostheses. Chow[3,4] and Zrenner[5,6] pioneered subretinal prostheses that implant the electrode array inside the subretinal space, followed by the development of epiretinal prostheses.[7–10] We are trying to develop suprachoroidal prostheses, in which the electrode array is positioned in neither the epiretinal nor the subretinal space but inside the sclera.[11] Compared with other aproaches, our suprachoroidal approach is advantageous because electrodes can be implanted by relatively low invasive surgery.[12] Therefore, our electrode array must satisfy the following two criteria. First, the size of the electrode array should be small enough to be inserted into the scleral flap. Second, each electrode should be able to deliver enough charge to stimulate retinal cells safely. In addition, our in vivo preliminary study has shown that a convex electrode is preferable to a planar electode. The fabrication of a convex electrode is difficult compared with conventional micromachining-based planar electrodes.[13,14]

It has been reported that the minimum threshold current amplitude is 100 μA for cathodic-first (CF) 500-μs-duration pulses to evoke electrically-evoked cortical potentials in rats.[11] We have assumed a safety coefficient of two for the current amplitude; therefore, the electrode should be able to inject current pulses of 200 μA amplitude and 500 μs duration safely. The charge delivery capability (CDC) of platinum is reported to be in the range of 300–350 μC/real cm^2, depending on the pulse polarity.[15] Assuming a CDC for platinum of 350 μC/cm^2, a 191-μm-diameter electrode is necessary to inject a pulse of 200 μA amplitude and a 500 μs width. This is why we set our development target to be 200-μm-diameter electrodes that can deliver CF biphasic pulses of 200 μA amplitude and 500 μs duration, which is equivalent to a charge density of 318 μC/cm^2. In this article we report on a fabrication process that accommodates convex electrodes and on the CDC measurements of our multichannel electrodes designed for intrascleral implantation. Then we discuss whether our electrodes satisfy our development target.

Received: January 4, 2006 / Accepted: August 16, 2006

Y. Terasawa (✉) · A. Uehara · T. Saitoh · M. Ozawa
Vision Institute, Nidek Co, Ltd, 73-1 Hama-cho, Gamagori 443-0036, Japan
Tel. +81-533-68-1815; Fax +81-533-68-1816
e-mail: yasuo_terasawa@nidek.co.jp

H. Tashiro
Department of Medicine, Kyushu University, Fukuoka, Japan

T. Tokuda · J. Ohta
Graduate School of Materials Science, Nara Institute of Science and Technology, Nara, Japan

Conclusion

We succeeded in fabricating a 10 × 10 bump-shaped electrode array onto a flexible substrate. CDC measurements of the electrodes indicated that 80% of electrodes (four of five) performed beyond 318 $\mu C/cm^2$, which was our development target. The fact that there was little difference between measured and target CDCs suggested the necessity of enhancing the charge delivery capability of electrodes.

Acknowledgments This work was supported by the New Energy Development Organization (NEDO) of Japan.

References

1. Santos A, Humayun MS, de Juan E Jr, Greenberg R, Marsh MJ, Klock IB, Milam AH. Preservation of the inner retina in retinits pigmentosa. A morphometric analysis. Arch Ophthalmol 1997;115: 511–515
2. Kim SY, Sadda S, Pearlman J, Humayun MS, de Juan E Jr, Melia BM, Green WR. Morphometric analysis of the macula in eyes with disciform age-related macular degeneration. Retina 2002;22:471–477
3. Chow AY, Chow VY. Subretinal electrical stimulation of the rabbit retina. Neurosci Lett 1997;225:13–16
4. Chow AY, Pardue MT, Chow VY, Peyman GA, Liang C, Perlman JI, Peachey NS. Implantation of silicon chip microphotodiode arrays into the cat subretinal space. IEEE Tran Neural Sys Rehab Eng 2001;9:86–95
5. Zrenner E, Stett A, Weiss S, Aramant RB, Guenther E, Kohler K, Miliczek KD, Seiler MJ, Haemmerle H. Can subretinal microphotodiodes successfully replace degenerated photoreceptors? Vision Res 1999;39:2555–2567
6. Stett A, Barth W, Weiss S, Haemmerle H, Zrenner E. Electrical multisite stimulation of the isolated chicken retina. Vision Res 2000;40:1785–1795
7. Humayun MS, de Juan E Jr, Weiland JD, Dagnelie G, Katona S, Greenberg R, Suzuki S. Pattern electrical stimulation of the human retina. Vision Res 1999;39:2569–2576
8. Humayun MS, Weiland JD, Fujii GY, Greenberg R, Williamson R, Little J, Mech B, Cimmarusti V, Boemel G, Dagnelie G, de Juan E Jr. Visual perception in a blind subject with a chronic microelectronic retinal prosthesis. Vision Res 2003;43:2573–2581
9. Laube T, Schanze T, Brockmann C, Bolle I, Stieglitz T, Bornfeld N. Chronically implanted epidural electrodes in Göttinger minipigs allow functional tests of epiretinal implants. Grafe's Arch Clin Exp Ophthalmol 2003;241:1013–1019
10. Walter P, Heimann K. Evoked cortical potentials after electrical stimulation of the inner retina in rabbits. Grafe's Arch Clin Exp Ophthalmol 2000;238:315–318
11. Kanda H, Morimoto T, Fujikado T, Tano Y, Fukuda Y, Sawai H. Electrophysiological studies of the feasibility of suprachoroidal-transretinal stimulation for artificial vision in normal and RCS rats. Invest Ophthalmol Vis Sci 2004;45:560–566
12. Nakauchi K, Fujikado T, Kanda H, Morimoto T, Choi JS, Ikuno Y, Sakaguchi S, Kamei M, Ohji M, Yagi T, Nishimura S, Sawai H, Fukuda Y, Tano Y. Transretinal electrical stimulation by an intrascleral multichannel electrode array in rabbit eyes. Grafe's Arch Clin Exp Ophthalmol 2005;243:169–174
13. Sieglitz T, Beutel H, Meyer JU. A flexible, light-weight multichannel sieve electrode with integrated cables for interfacing regenerating peripheral nerves. Sensors Actuators A 1997;60: 240–243
14. Rizzo JF III, Wyatt J, Lowenstein J, Kelly S, Shire D. Methods and perceptual thresholds for short-term electrical stimulation of human retina with microelectrode arrays. Invest Ophthalmol Vis Sci 2003;44;5355–5361
15. Brummer SB, Turner MJ. Electrical stimulation with Pt electrodes: II Estimation of maximum surface redox (theoretical non-gassing) limits. IEEE Trans Biomed Eng 1977;24:440–443
16. Tokuda T, Pan YL, Uehara A, Kagawa K, Nunoshita M, Ohta J. Flexible and extendible neural interface device based on cooperative multi-chip CMOS LSI architecture. Sensors Actuators A 2005;122:88–98
17. Licari JJ. Coating materials for electronic applications. New York: Noyes, 2003
18. Wolgemuth L. The surface modification properties of parylene for medical applications. Business Brief Med Device Manuf Technol 2002;1–4
19. Noh HS, Huang Y, Hesketh PJ. Parylene micromolding, a rapid and low-cost fabrication method for parylene microchannels. Sensors Actuators B 2004;102:78–85
20. Brummer SB, Turner MJ. Electrochemical considerations for safe electrical stimulation of the nervous system with platinum electrodes. IEEE Trans Biomed Eng 1977;24:59–63
21. Rose TL, Robblee LS. Electrical stimulation with Pt electrodes. VIII. Electrochemically safe charge injection limits with 0.2-ms pulses. IEEE Trans Biomed Eng 1990;37:1118–1120
22. Brummer SB, Turner MJ. Electrical stimulation with Pt electrodes: I A method for determination of "real" electrode areas. IEEE Trans Biomed Eng 1977;24:436–439
23. Kelliher EM, Rose TL. Evaluation of charge injection properties of thin film redox materials for use as neural stimulation. Mat Res Soc Symp Proc 1989;110:23–27
24. Cogan SF, Troyk PR, Ehrlich J, Plante TD. In vitro comparison of the charge-injection limits of activated iridium oxide (AIROF) and platinum-iridium microelectrodes. IEEE Trans Biomed Eng 2005; 52:1612–1614
25. Weiland JD, Anderson DJ, Humayun MS. In vitro electrical properties for iridium oxide versus titanium nitride stimulating electrodes. IEEE Trans Biomed Eng 2002;49:1574–1579
26. Beebe X, Rose TL. Charge injection limits of activated iridium oxide electrodes with 0.2-ms pulses in bicarbonate buffered saline. IEEE Trans Biomed Eng 1988;35:494–495
27. Janders M, Egert U, Stelze M, Nisch W. Novel thin-film titanium nitride microelectrodes with excellent charge transfer capability for cell stimulation and sensing applications. Proceedings of the 19th International Conference IEEE/EMBS. Piscataway: IEEE, 1996:1191–1193

Jpn J Ophthalmol 2006;50:53–61
© Japanese Ophthalmological Society 2006
DOI 10.1007/s10384-005-0270-4

13.

CLINICAL INVESTIGATION

Vitrectomy for Myopic Posterior Retinoschisis or Foveal Detachment

Akito Hirakata and Tetsuo Hida

Kyorin Eye Center, Kyorin University School of Medicine, Mitaka, Tokyo, Japan

Abstract

Purpose: To evaluate the efficacy of vitrectomy for posterior retinoschisis (RS) or foveal detachment (FD) associated with posterior staphyloma in myopic eyes.

Methods: We reviewed the records of 14 consecutive patients (53–77 years of age; 16 eyes) with progressive visual impairment as a result of myopic RS or FD. Optical coherence tomography demonstrated the presence of a variety of RS and FD characteristics. Five eyes had RS alone, and 11 eyes had RS and FD. Two eyes with RS and severe FD developed retinal detachment in conjunction with a tiny macular hole. Vitrectomy, including posterior vitreous separation in all eyes and internal limiting membrane (ILM) peeling in six eyes, had been performed. The patients were followed postoperatively for 6 to 66 months (mean, 24 months). The anatomical outcome and visual acuity were retrospectively analyzed in this study.

Results: Although the two eyes with RS and severe FD developed retinal detachment with a macular hole after an initial vitrectomy, final retinal reattachment was achieved in all 16 eyes. Visual acuity improved in nine eyes and remained unchanged in seven eyes.

Conclusions: Vitrectomy with posterior vitreous separation is effective for reattaching the macula and preventing a deterioration of vision, although eyes with RS and severe FD may be at risk for the development of a macular hole after the initial vitrectomy. **Jpn J Ophthalmol** 2006;50:53–61 © Japanese Ophthalmological Society 2006

Key Words: high myopia, macular detachment, optical coherence tomography, retinoschisis, vitrectomy

Introduction

Posterior retinal detachment associated with a macular hole is a well-known complication in highly myopic eyes with posterior staphyloma. However, localized shallow posterior retinal detachment inside posterior staphyloma can also exist in the absence of a macular hole. In 1958, Phillips noted that localized posterior retinal detachment over posterior staphyloma might occur in the absence of a retinal hole.[1] Using optical coherence tomography (OCT), Takano and Kishi[2] reported that foveal retinoschisis or foveal retinal detachment occurs frequently in severely myopic eyes with posterior staphyloma, even in the absence of a macular hole. They suggested that retinal detachment may precede the formation of a macular hole in highly myopic eyes. However, the pathological mechanism responsible for posterior retinoschisis and the process of macular hole development are not well understood.

Recently, several authors have reported that vitrectomy, internal limiting membrane (ILM) peeling, and gas tamponade are useful for the treatment of foveal retinoschisis in highly myopic eyes.[3–7] Kobayashi and Kishi[4] also suggested that vitreous surgery might be indicated as a prophylactic treatment in highly myopic eyes at high risk for macular hole development. However, myopic foveal retinoschisis exhibits a variety of profiles,[8,9] and the accumulated data on surgical cases remain insufficient to prove

Received: October 12, 2004 / Accepted: May 2, 2005
Correspondence and reprint requests to: Akito Hirakata, Department of Ophthalmology, Kyorin University School of Medicine, 6-20-2 Shinkawa, Mitaka, Tokyo 181-8611, Japan
e-mail: hirakata@eye-center.org

Jpn J Ophthalmol
Vol 50: 53–61, 2006

whether vitrectomy is effective for the alleviation of this condition.

The purpose of the present study was to examine the clinical outcomes of vitrectomies performed in the Kyorin University Hospital between September 1998 and February 2004 in 14 consecutive patients (16 eyes) with localized shallow posterior retinal detachment inside a posterior staphyloma who exhibited signs of progressive visual impairment. Different clinical terms have been used to describe this pathological condition in previous reports, including foveal retinoschisis,[2] foveal detachment and retinoschisis,[2,4] macular retinoschisis,[5,9] shallow detachment of the macula,[1] and foveal retinal detachment without a macular hole.[8] In this paper, we use the terms posterior retinoschisis (RS) and foveal detachment (FD) to describe this pathological condition.

Patients and Methods

Fourteen consecutive patients (16 eyes) with myopia and posterior staphyloma who exhibited progressive visual impairment as a result of RS or FD were included in this study. Their records were retrospectively reviewed. Informed consent had been obtained from all study patients. The fundus of each patient had been pre- and postoperatively examined by indirect ophthalmoscopy and slit-lamp biomicroscopy using a Goldmann contact lens and a 90-diopter noncontact fundus examination lens (SuperField Lens). The best-corrected visual acuity (BCVA) was recorded. An OCT system (Zeiss-Humphrey, San Leandro, CA, USA) had been used to observe the posterior retinal changes. In this study the anatomical outcome and BCVA were retrospectively analyzed for all eyes.

Surgery had been initiated once the patient's vision had begun to deteriorate and the macular detachment had persisted or progressed for 3 months or longer. Two eyes (cases 13, 14) with RS and severe FD developed retinal detachment with a tiny macular hole before the vitrectomy. All the operations were performed by the same surgeon (AH) between September 1998 and February 2004. Vitrectomy, including posterior vitreous cortex removal from the retinal surface, was performed in all eyes, and ILM peeling was performed in six eyes. After core vitrectomy, complete removal of the posterior vitreous cortex (typically appearing as a thin membrane) from the posterior retinal surface was initiated by cutting with a microvitreoretinal knife (20-gauge) or a diamond-dusted membrane scraper.[10] A viscodissection technique[11] was used to advance the posterior hyaloid separation gently over the areas of retinoschisis in the posterior staphyloma. Triamcinolone acetonide (TA) was used intraoperatively in five cases to highlight the posterior hyaloid membrane.[12] ILM peeling over the posterior pole was regarded as indicated in eyes in which the presence of posterior hyaloid separation or induction over the macula was uncertain during the vitreous surgery, and was performed after indocyanine green (ICG) staining (5 mg/ml) in six eyes. In 12 eyes, fluid–air exchange was carried out without drainage of the subretinal fluid, followed by gas tamponade with either 20% sulfur hexafluoride (SF_6) or 14% perfluoropropane (C_3F_8). The patients were placed in a facedown position postoperatively. In two eyes [patients 5 (right eye, R) and 10], silicone oil tamponade was used because of poor vision in the opposite eye.

Twelve eyes were phakic before surgery, and four eyes had received phacoemulsification with intraocular lens implantation for the treatment of senile cataracts. Among the 12 phakic eyes, phacoemulsification with intraocular lens implantation was performed simultaneously with the vitrectomy in two eyes, and after the vitrectomy in six eyes.

The patients were followed for 6 to 66 months (mean, 24 months) after surgery.

Results

Case Reports

Patient 1

A 59-year-old man presented with a history of several months of metamorphopsia in his right eye. He also had a

Figure 1A–C. Fundus photograph and optical coherence tomography (OCT) images of the right eye of patient 1. A A photograph taken at presentation in an eye with a best-corrected visual acuity (BCVA) of 0.5 and metamorphopsia shows a shallow macular detachment over the posterior staphyloma. B An OCT examination confirmed the foveal detachment and posterior retinoschisis (scan length, 5.0 mm). C About 4 years after the operation, the BCVA had improved to 0.7. An OCT image shows complete reattachment (scan length, 5.0 mm).

Figure 2A–D. Fundus photograph and OCT images of the right eye of patient 2. A During a routine follow-up for macular hole retinal detachment in the left eye, the BCVA of the right eye was found to have decreased from 0.8 to 0.5. The fundus photograph shows a shallow macular detachment. B A preoperative OCT image shows a shallow elevation of the macula without splitting of the fovea, creating the appearance of a lamellar hole (scan length, 5.0 mm). C Two months after the vitrectomy, an OCT image shows a marked resolution of the retinoschisis (scan length, 3.5 mm). D At 4 years postoperatively, the retina had completely reattached (scan length, 10.0 mm).

Figure 3A–C. Fundus photograph and OCT images of the right eye of patient 11. A A preoperative fundus photograph shows a shallow retinal elevation over a posterior staphyloma in an eye with a BCVA of 0.4. B A preoperative OCT image shows an inner layer separation that appears to be connected to the conus of the optic disc (1), as well as to a large outer layer detachment at the macula (2). A partial posterior hyaloid separation surrounding the posterior retinoschisis is visible (scan length, 10.0 mm). C At 6 months after the vitrectomy, an OCT image shows a marked improvement of the retinal detachment (scan length, 10.0 mm).

Figure 4A–C. Fundus photograph and OCT images of the left eye of patient 5. A A preoperative fundus photograph shows a shallow retinal elevation over a posterior staphyloma. The BCVA of the eye was 0.06. B An OCT image shows a posterior retinoschisis over the posterior staphyloma, with a partial separation of the posterior hyaloid. Outer layer detachment is not visible (scan length, 10.0 mm). C Two weeks after the vitrectomy, the retina had completely reattached (scan length, 10.0 mm).

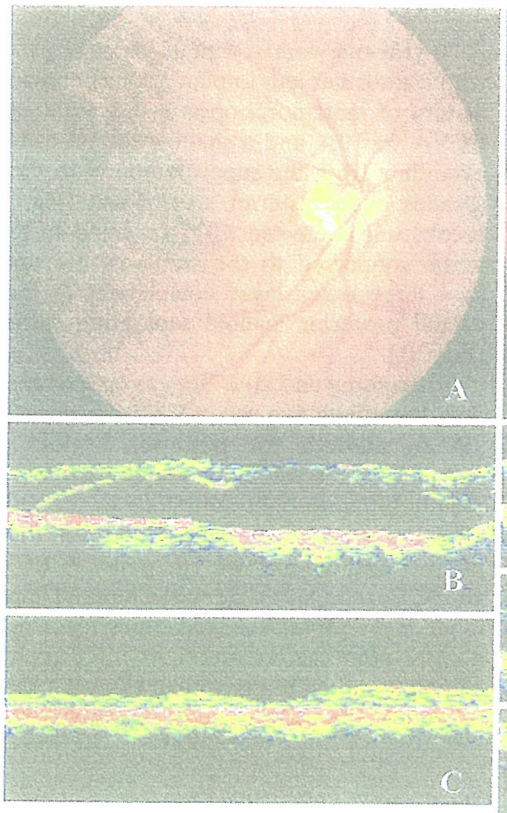

Figure 1

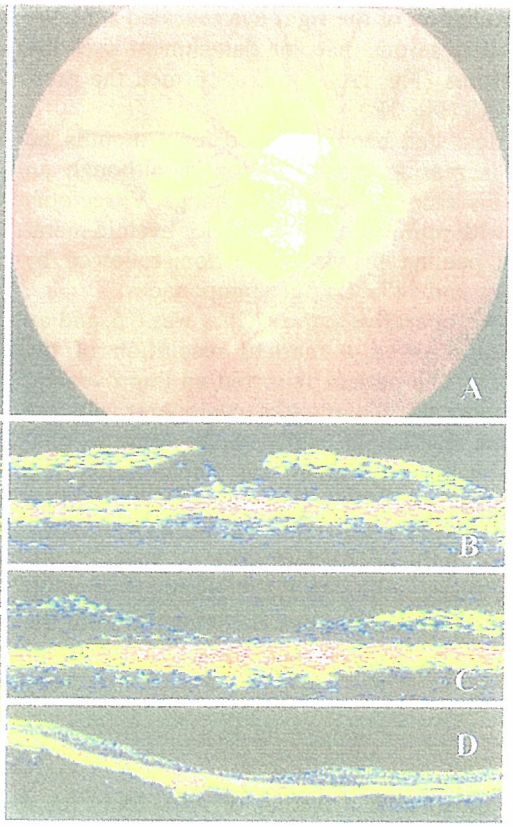

Figure 2

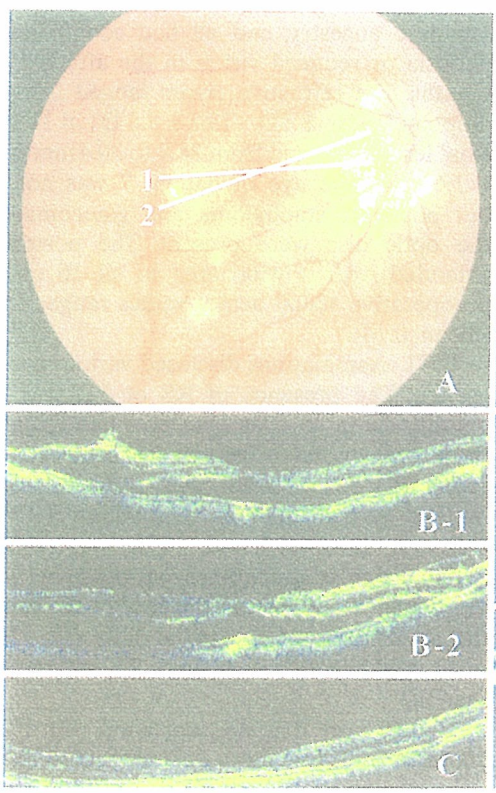

Figure 3

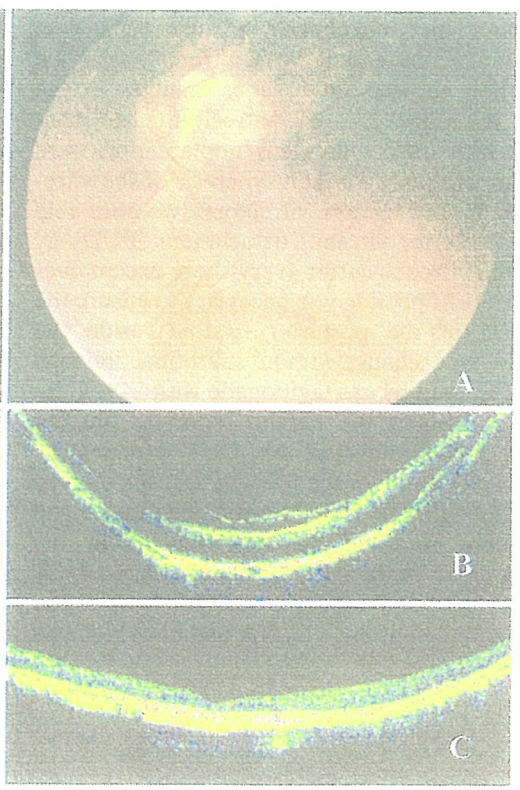

Figure 4

history of von Recklinghausen disease and refractive amblyopia. Examination of the right eye revealed a BCVA of 0.5 and a shallow serous macular detachment over the posterior staphyloma (Fig. 1A). OCT confirmed the presence of FD and RS (Fig. 1B).

After the patient had been observed for 3 months, he complained of increasing metamorphopsia, although an examination of his vision revealed no change. Vitrectomy was performed, with removal of the posterior hyaloid membrane and ILM peeling by viscodissection, followed by air–fluid exchange and 14% C_3F_8 gas tamponade.

Two months postoperatively, the BCVA was 0.6, and an OCT examination showed a marked resolution of the retinal detachment. The patient reported an improvement in the metamorphopsia. Six months postoperatively, the patient developed nuclear sclerosis of the lens, so phacoemulsification with intraocular lens implantation was performed. Consequently, the patient's BCVA further improved to 0.7. The posterior retina was found to be completely reattached, with no further changes during a 54-month follow-up examination. An OCT examination about 4 years later revealed a nearly normal configuration of the fovea (Fig. 1C).

Patient 2

A 53-year-old woman with a history of vitrectomy for a macular hole retinal detachment in her left eye 3 years earlier was noted to have a shallow elevation of the macula in her asymptomatic right eye during a routine follow-up examination. OCT revealed RS in the right eye.

One year later, she complained of a slight decrease in central vision and metamorphopsia in her right eye. Although her visual acuity had decreased from 0.8 to 0.4, a fundus examination showed no obvious changes in the severity of the RS (Figs. 2A, B). Vitrectomy and phacoemulsification with intraocular lens implantation were performed. Intraoperatively, marked syneresis of the vitreous was observed. Following core vitrectomy, we were able to easily induce posterior vitreous detachment (PVD) by suctioning with the vitreous cutter everywhere except over the posterior pole; ILM peeling was necessary to ensure the complete removal of the posterior hyaloid inside the staphyloma. Fluid–air exchange without subretinal drainage was performed, followed by gas tamponade with 14% C_3F_8. Two months after surgery, the patient reported that her metamorphopsia had diminished. An OCT examination showed a marked resolution of the RS (Fig. 2C). Six months after surgery, although the BCVA remained unchanged at 0.5, the patient reported an improvement in the metamorphopsia. Four years after the operation, an OCT examination confirmed the complete reattachment of the retina (Fig. 2D), and the patient's BCVA had been restored to 0.8.

Patient 11

A 70-year-old woman with a history of phacoemulsification with intraocular lens implantation complained of a 4-month history of metamorphopsia in her right eye. The patient's BCVA was 0.4, and a shallow retinal elevation was noted extending from the superotemporal to the inferotemporal arcades over posterior staphyloma (Fig. 3A). No retinal breaks were detected. OCT revealed an RS that appeared to be connected to the conus of the optic disc, as well as a large outer layer detachment at the macula and a partial posterior hyaloid separation surrounding the RS (Fig. 3B).

Vitrectomy and 20% SF_6 gas tamponade was performed with the adjunctive use of TA intraoperatively. The use of TA to observe the posterior hyaloid intraoperatively appears to be a useful technique when attempting to completely separate tight adhesions to the retina. One month after the surgery, the patient reported that her metamorphopsia had diminished. The patient's BCVA was 0.5, and an OCT examination showed a marked improvement in the inner layer separation and outer layer detachment. At 6 months after the operation, an OCT examination showed complete retinal reattachment (Fig. 3C). One year after the operation, the BCVA had been restored to 0.7.

Preoperative Clinical Characteristics

The clinical characteristics of all 14 patients are shown in Table 1. Eleven patients were women and three were men, and they ranged in age from 53 to 77 years (mean ± SD, 64.8 ± 7.7 years). All the patients were healthy and of Japanese ancestry, and all had complained of metamorphopsia or reduced vision in the affected eye for several months. The refractive errors ranged from −6.0 to −19.25 diopters (mean ± SD, −13.2 ± 3.8 D) in 12 phakic eyes. The axial lengths ranged from 24.9 to 30.4 mm (mean ± SD, 27.6 ± 1.6 mm). The eye of patient 7 was not highly myopic, but posterior staphyloma and glaucomatous cupping of the optic disc were present. The posterior staphyloma extended over a wide area in all 16 eyes. The decimal preoperative visual acuity values ranged from 0.01 to 0.5 (mean, 0.14).

OCT examinations disclosed various profiles of macular change. The presence of RS or FD was confirmed preoperatively in all eyes. Five eyes had RS alone. In four of these eyes, an extensive hyporefractive space had split the retina into a thick inner layer and a thin outer layer lying on the retinal pigment epithelium (RPE) [patients 1 (left eye, L), 3, 5 (R), and 6] (Fig. 4A, B). One eye (patient 2) had a similar appearance, but the fovea was not split and did not show a defect in the roof of the central cyst, giving the appearance of a lamellar hole (Fig. 2B). The BCVA in four of the five eyes with RS without FD was better than 0.2.

Eleven eyes had RS associated with FD (Figs. 1B, 3B, 5B). The BCVA of these eyes seemed to be worse than that

Table 1. Clinical characteristics

Patient	Age (years)	Sex	Eye	Ref (D)	Axial length (mm)	Symptom	Preoperative BCVA	OCT finding		Intraoperative finding				Final BCVA	Complications	Follow-up (months)	Fellow eye
								RS/FD	PVD	PVD Ind.	ILM peel	Tamp	Final attachment				
1	59	M	L	−8.75	26.7	Decreased VA	0.06	RS	—	+	−	C_3F_8	+	0.2	—	66	RS,FD
			R	−11.00	27.0	Decreased VA	0.5	RS,FD	—	+	+	C_3F_8	+	0.7	—	54	RS
2	53	F	R	−19.25	28.7	Metamorphopsia	0.4	RS	—	+	+	C_3F_8	+	0.8	—	52	MHRD
3	72	F	R	−9.75	27.9	Metamorphopsia	0.4	RS	—	+	+	—	+	0.8	—	45	—
4	75	F	R	IOL	26.2	VF defect	0.01	RS,FD	—	+	+	C_3F_8	+	0.07	MH	17	—
5	68	F	L	−15.00	27.5	Decreased VA	0.06	RS,FD	Part	+	−	SF_6	+	0.06	RRD	16	RS
			R	−17.75	30.0	Metamorphopsia	0.2	RS	Part	+	−	SO	+	0.6	Retinal break	10	RS,FD
6	63	F	L	−12.5	29.2	Metamorphopsia	0.4	RS	—	+	−	—	+	0.4	—	27	—
7	63	M	L	−6.0	24.9	Decreased VA	0.1	RS,FD	—	+	+	SF_6	+	0.5	—	27	Gla
8	54	F	R	−15.00	27.0	Metamorphopsia	0.01	RS,FD	Part	+	+	SF_6	+	0.1	MHRD	22	—
9	56	F	L	−14.00	29.2	Decreased VA	0.2	RS,FD	Part	+	−	SF_6	+	0.1	MHRD	17	RS,FD
10	77	F	L	IOL	27.4	Metamorphopsia	0.3	RS,FD	Part	+	−	SO	+	0.3	—	15	MHRD
11	70	F	R	IOL	30.2	Metamorphopsia	0.4	RS,FD	Part	+	−	SF_6	+	0.7	—	13	—
12	74	F	R	IOL	29.9	VF defect	0.06	RS,FD	Part	+	−	SF_6	+	0.2	—	6	RS
13	66	M	L	−15.00	29.6	Decreased VA	0.3→0.1	RS,FD→MHRD	—	+	−	C_3F_8	+	0.2	MH	11	MHRD
14	59	F	R	−19.00	30.4	Decreased VA	0.2→0.06	RS,FD→MHRD	—	+	−	C_3F_8	+	0.4	MH	12	—

BCVA, best-corrected visual acuity; C_3F_8, perfluoropropane; D, diopter; F, female; FD, foveal detachment; Gla, glaucoma; ILM, internal limiting membrane; Ind, induction; IOL, intraocular lens; L, left; M, male; MH, macular hole; MHRD, macular hole retinal detachment; OCT, optical computed tomography; Part, partial detachment; PVD, posterior vitreous detachment; R, right; Ref, refractive error; RRD, rhegmatogenous retinal detachment; RS, retinoschisis; SO, silicone oil; SF_6, sulfur hexafluoride; Tamp, tamponade; VA, visual acuity; VF, visual field.

of the eyes without FD, but 6 of the 11 eyes with FD had a BCVA that was better than 0.2. Two eyes developed macular hole retinal detachment during the routine follow-up period, and the BCVA decreased from 0.3 to 0.1 in patient 13 and from 0.2 to 0.06 in patient 14. Figures 6 and 7 show the changes in the macular configurations associated with the reduction in BCVA during the follow-up period in patients 13 and 14.

The presence of a partially detached posterior hyaloid was disclosed in seven eyes (Figs. 3, 4, 5). The separation of the posterior hyaloid beside the conus of the optic disc was observed in all of these seven eyes. Advanced vitreous syneresis was observed in all of these eyes, but PVD was not observed in the other nine eyes preoperatively.

Regarding the fellow eyes of the patients, three patients had a medical history of macular hole detachment, five patients had a history of RS and/or FD, one patient had a history of myopic posterior chorioretinal atrophy, and one patient had a history of primary open-angle glaucoma.

Anatomical Results

In all five eyes that had RS without FD, the retina reattached after the initial vitrectomy. Retinal reattachment was achieved in 8 out of 11 eyes with both RS and FD, including two cases that had progressed to macular hole retinal detachment (patients 13 and 14) before the initial vitrectomy. We removed the silicone oil about 5 and 2 months after the vitrectomies in patients 5 (R) and 10, respectively. The retina remained reattached after the removal.

Three eyes required reoperation because of recurrent retinal detachment. In two of these three eyes, a full-thickness macular hole associated with posterior retinal detachment occurred 1 month after vitrectomy with (patient 8) and without ILM peeling (patient 9; Fig. 8). We performed a second operation, consisting of extensive ILM peeling and silicone oil tamponade. At 5 months (patient 8) and 3 months (patient 9) after the second surgery, we removed the silicone oil, and retinal reattachment was confirmed by OCT in both eyes. One eye (patient 5, L) developed retinal detachment caused by a peripheral retinal break immediately after the initial vitrectomy. A second vitrectomy was thus performed to repair the retinal detachment.

Final retinal reattachment was achieved in all 16 eyes. No recurrences were observed during follow-up.

Visual Acuity Results

An improvement in the BCVA of 0.2 logMAR or greater was documented in 9 of the 16 eyes. The BCVA of seven eyes remained unchanged. The BCVA of the left eye of patient 5 improved from 0.06 to 0.1 at 12 months after the vitrectomy, but decreased again to 0.06 at 16 months, with no remarkable changes in the retinal findings. During this follow-up period, we performed a vitrectomy for the treat-

Jpn J Ophthalmol
Vol 50: 53–61, 2006

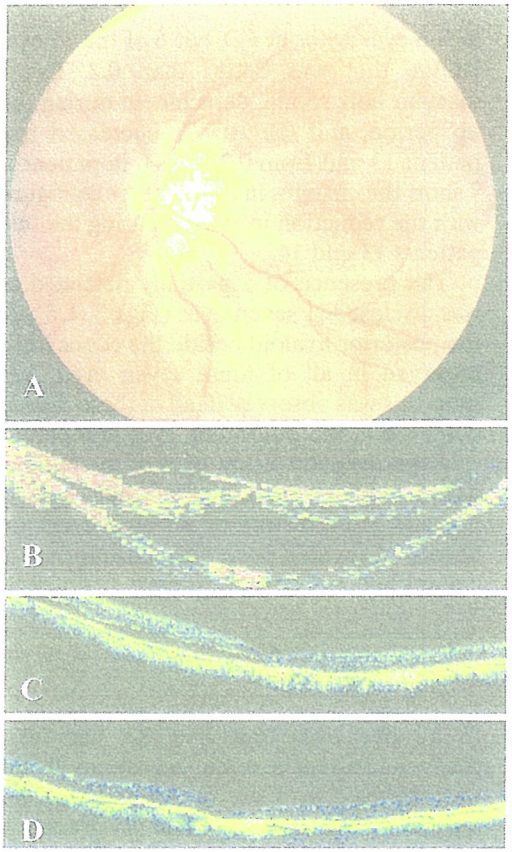

Figure 5

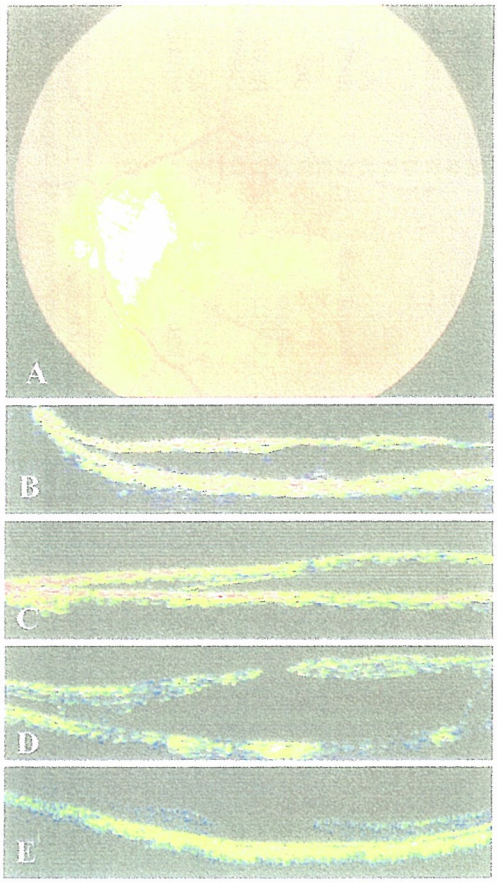

Figure 6

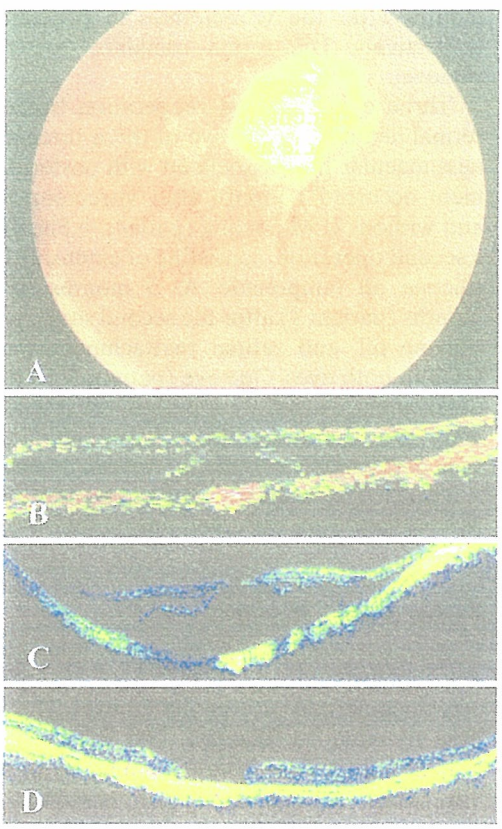

Figure 7

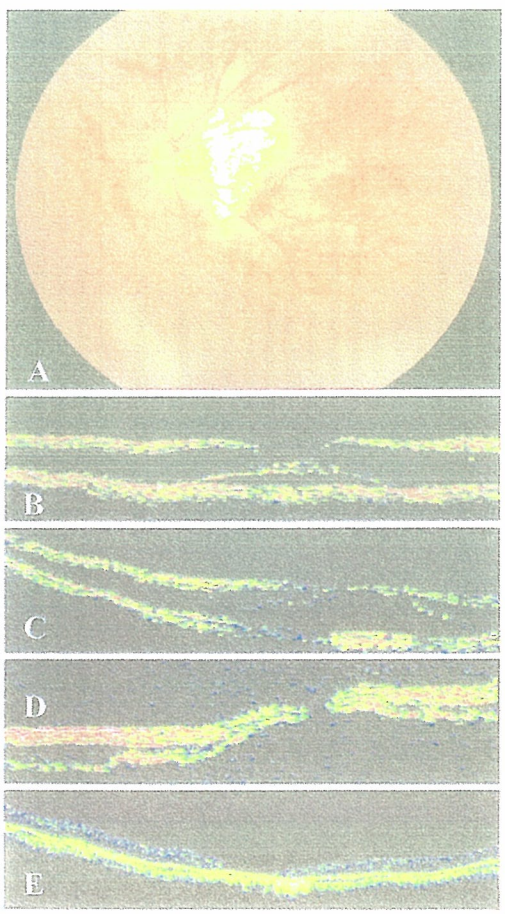

Figure 8